


Fabrication of Rosuvastatin-Incorporated Polycaprolactone -Gelatin Scaffold for Bone Repair: A Preliminary *In Vitro* Study

Maliheh Gharibshahian, Ph.D.¹, Morteza Alizadeh, Ph.D.², Mohammad Kamalabadi Farahani, Ph.D.²,
Majid Salehi, Ph.D.^{2, 3, 4*} 

1. Student Research Committee, School of Medicine, Shahrood University of Medical Sciences, Shahrood, Iran
2. Department of Tissue Engineering, School of Medicine, Shahrood University of Medical Sciences, Shahrood, Iran
3. Tissue Engineering and Stem Cells Research Centre, Shahrood University of Medical Sciences, Shahrood, Iran
4. Sexual Health and Fertility Research Centre, Shahrood University of Medical Sciences, Shahrood, Iran

Abstract

Objective: Rosuvastatin (RSV) is a hydrophilic, effective statin with a long half-life that stimulates bone regeneration. The present study aims to develop a new scaffold and controlled release system for RSV with favourable properties for bone tissue engineering (BTE).

Materials and Methods: In this experimental study, high porous polycaprolactone (PCL)-gelatin scaffolds that contained different concentrations of RSV (0 mg/10 ml, 0.1 mg/10 ml, 0.5 mg/10 ml, 2.5 mg/10 ml, 12.5 mg/10 ml, and 62.5 mg/10 ml) were fabricated by the thermally-induced phase separation (TIPS) method. Mechanical and biological properties of the scaffolds were evaluated by Fourier transform infrared spectroscopy (FTIR), scanning electron microscope (SEM), compressive strength, porosity, MTT, alkaline phosphatase (ALP) activity, water contact angle, degradation rate, pH alteration, blood clotting index (BCI), and hemocompatibility.

Results: SEM analysis confirmed that the porous structure of the scaffolds contained interconnected pores. FTIR results showed that the RSV structure was maintained during the scaffold's fabrication. RSV (up to 62.5 mg/10 ml) increased compressive strength (16.342 ± 1.79 MPa), wettability (70.2), and degradation rate of the scaffolds. Scaffolds that contained 2.5 mg/10 ml RSV had the best effect on the human umbilical cord mesenchymal stem cell (HUC-MSCs) survival, hemocompatibility, and BCI. As a sustained release system, only $31.68 \pm 0.1\%$ of RSV was released from the PCL-Gelatin-2.5 mg/10 ml RSV scaffold over 30 days. In addition, the results of ALP activity showed that RSV increased the osteogenic differentiation potential of the scaffolds.

Conclusion: PCL-Gelatin-2.5 mg/10 ml RSV scaffolds have favorable mechanical, physical, and osteogenic properties for bone tissue and provide a favorable release system for RSV. They can be mentioned as a promising strategy for bone regeneration that should be further assessed in animals and clinical studies.

Keywords: Bone, Gelatin, Polycaprolactone, Regeneration, Rosuvastatin

Citation: Gharibshahian M, Alizadeh M, Kamalabadi Farahani M, Salehi M. Fabrication of rosuvastatin-incorporated polycaprolactone -gelatin scaffold for bone repair: a preliminary in vitro study. Cell J. 2024; 26(1): 70-80. doi: 10.22074/CELLJ.2023.2009047.1391
This open-access article has been published under the terms of the Creative Commons Attribution Non-Commercial 3.0 (CC BY-NC 3.0).

Introduction

One of the vital clinical needs of tissue engineering is the reconstruction of fractures and congenital and trauma-induced bone defects that are larger than the critical size. These fractures and defects can lead to permanent functional disability if they do not fully heal (1). Tissue engineering can be used to design and manufacture biodegradable and biocompatible scaffolds in combination with various types of cells and biochemical agents to stimulate local bone formation and decrease healing time (2). The selection of appropriate materials is one of the main requirements to encourage optimal osteoblastic adhesion and differentiation for bone scaffolds (3, 4).

Various polymers are used in bone tissue engineering (BTE). Among them, polycaprolactone (PCL) is a

linear aliphatic polyester and a hydrophobic synthetic polymer approved by the United States Food and Drug Administration that has attracted much attention (5). PCL is a biocompatible, flexible, thermoplastic, and biodegradable polymer. It has suitable stiffness and mechanical properties for bone applications. This polymer is affordable, easy to process, not carcinogenic, and has low immunogenicity. However, due to the slow degradation rate of PCL (about 2-4 years), lack of osteogenesis potential, and its hydrophobic nature, the PCL composite is generally used with other polymers and growth factors (6, 7).

Gelatin is a natural, hydrophilic polymer obtained from the incomplete hydrolysis of collagen. Properties of this polymer include low antigenicity, rapid degradation, favourable biocompatibility, availability,

Received: 11/August/2023, Revised: 16/November/2023, Accepted: 05/December/2023

*Corresponding Address: P.O.Box: 3614773943, Department of Tissue Engineering, School of Medicine, Shahrood University of Medical Sciences, Shahrood, Iran

Email: Salehi.m@shmu.ac.ir



cost-effectiveness, and the presence of an Arg–Gly–Asp (RGD) sequence (7, 8). Gelatin reinforces cell adhesion due to these RGD sequences. Although gelatin has good cell adhesion, proliferation and differentiation properties (9), its use in tissue engineering applications has been restricted by low mechanical strength and rapid breakdown (7).

Statins are specific inhibitors of 3-hydroxy-2-methylglutaryl coenzyme A (HMG-CoA) reductase (an enzyme that limits the rate of cholesterol synthesis) that play a role in the treatment of hyperlipidaemia and atherosclerosis. Various studies have reported the effects of statins for osteoporosis, angiogenesis, osteogenesis, and modulation of inflammation (10, 11). Rosuvastatin (RSV) is a group of second-generation hydrophilic statins that play a role in reducing fat and preventing cardiovascular disorders (12). Due to its hydrophilic nature, RSV does not easily penetrate the bilayer lipid membrane of the cell and needs special carriers to enter the cells. In addition to its anti-inflammatory effects, RSV can stimulate osteogenesis, differentiate osteoblastic cells, and reduce oxidative stress (13). This statin helps to reduce inflammation by increasing nitric oxide production and inhibiting phosphorus selectin synthesis (14). RSV decreases the activity of osteoclasts, stimulates the differentiation of osteoblasts, and increases bone mineralisation. It increases bone morphogenetic protein (BMP)-2 expression and alkaline phosphatase (ALP) activity (10). BMP-2, as a bone-inducing factor, helps bone formation by increasing the transcription of bone-inducing genes and stimulates the differentiation of immature mesenchymal cells, including osteoblasts. Therefore, their use will be more favourable than expensive growth factors with a short half-life that may lead to immune stimulation (due to high molecular weight) (10, 15).

Various studies have shown the effect of oral administration of RSV on bone repair; however, due to its primary metabolism in the liver and low bioavailability (less than 20%), oral use of RSV does not provide a suitable effect on bone formation and sometimes leads to autoimmune myopathy, rhabdomyolysis, nausea, and hepatic injury (10). Therefore, RSV should be incorporated into scaffolds/carriers to optimize its efficiency (16). Monjo et al. (13) used a collagen sponge that contained RSV and obtained the release of more than 50% of RSV within three hours. Rezazadeh et al. (15) applied chitosan/chondroitin sulphate nanoparticles that contained RSV and integrated these nanoparticles into a heat-sensitive Pluronic F127/hyaluronic acid hydrogel to create an optimal release system for RSV. Their results showed that more than 60% of the drug was released within 48 hours and had a positive effect on the survival and proliferation of osteoblasts in the culture medium. Ibrahim and Fahmy (17) used RSV-containing collagen sponges to repair bone defects created in rat femurs. They observed the formation of new bone with higher mineral density in the rats.

The thermally-induced phase separation (TIPS) method is a desirable technique for the fabrication of bone scaffolds with interconnected pores. The basis of this process is the use of a change in thermal energy to convert the thermodynamically homogeneous polymer solution into polymer- and solvent-rich phases. Finally, a porous structure with interconnected pores is fabricated by extracting the solvent (18). Scaffolds with different morphologies can be obtained by controlling various parameters of the TIPS method, such as polymer type, solvent type, polymer concentration, temperature, and solvent or non-solvent ratio (8).

The present study aims to fabricate a novel scaffold and release system for sustained release of RSV. For this purpose, we intend to fabricate a PCL-gelatin composite scaffold that contains different concentrations of RSV using the TIPS method and evaluate the role of various RSV concentrations on the physical, mechanical, and cell behaviour properties of these scaffolds. Our results can provide an acceptable platform for BTE research.

Materials and Methods

In this experimental study, the chemicals used for the fabrication of the scaffolds included: PCL (mw: 80 000 g/mol, Sigma-Aldrich Company, St. Louis, MO, USA), gelatin type B (mw: 180.155 g/mol, DNA Biotech Company, Tehran, Iran), and 1,4-dioxane (mw: 88.11 g/mol, DNA Biotech Company, Tehran, Iran).

The Ethical Committee of Shahrood University of Medical Sciences, Shahrood, Iran approved this research (IR.SHMU.REC.1401.078).

Scaffold preparation

The TIPS method was used to fabricate the scaffolds. For this purpose, we prepared a 5% (W/V) solution of PCL in 1,4-dioxane. Gelatin powder (25% W/W PCL) was added to the above solution. The resultant solution was stirred for 24 hours and sonicated for 20 minutes. Then, this homogenous solution was divided into six equal parts, and we separately added various amounts of RSV powder (0 mg/10 ml, 0.1 mg/10 ml, 0.5 mg/10 ml, 2.5 mg/10 ml, 12.5 mg/10 ml, and 62.5 mg/10 ml) to the solution. The solutions were stirred for 4 hours. In order to perform an optimal phase separation, the above solutions were flash-frozen below the dioxane freezing point in a nitrogen tank, stored at -80°C for 24 hours, and then freeze-dried for 48 hours to form porous scaffolds by solvent sublimation.

Scaffold characterization

Fourier transform infrared spectroscopy analysis

Functional groups or surface chemical bonds on the scaffolds and the stability of RSV during the fabrication process were analysed using Fourier transform infrared (FTIR) spectroscopy. For this purpose, an FTIR

spectrophotometer (WQF-510A, Rayleigh, China) was used at a wavelength range of 1000–4000 cm^{-1} .

Scanning electron microscope

The KYKY Technology scanning electron microscope (SEM, Beijing, China) was used to evaluate scaffold morphology. A coating of gold was applied on the scaffolds using a sputter cutter for 90 seconds at a current of 18 mA. Then, the samples were observed by SEM with an accelerating voltage of 18 kV. At least 20 random measurements and their frequencies in each SEM image were checked by the ImageJ software (National Institutes of Health, Bethesda, MD, USA) to determine the pore size.

Porosity assessment

The scaffolds were immersed in 10 ml of ethanol. Scaffold porosity was calculated using the liquid displacement method and the following equation:

$$\text{porosity} = (v_1 - v_3) / (v_2 - v_3) \times 100$$

Where V_1 is the initial volume of absolute ethanol, V_2 is the volume of ethanol after immersing the scaffold, and V_3 is the remaining volume of ethanol after removing the scaffold. Each scaffold was evaluated in triplicate (18).

Weight loss assessment

The biodegradability of the scaffolds was evaluated by measuring their weight loss after 30 days. Scaffolds that had the same dimension (1 cm^3) were weighed and immersed in 10 ml of phosphate-buffered saline (PBS) at 37°C. Then, at specified time points, the scaffolds were extracted from the PBS, dried, and weighed. The amount of weight loss was calculated using the following equation:

$$\text{Weight-loss (\%)} = (w_1 - w_2) / w_1 \times 100$$

Where W_1 is the initial weight of the sample, and W_2 is their dry weight after extraction from PBS. The average values of three samples were considered for each group (19).

Wettability evaluation

A static contact angle measuring device (KRÜSS GmbH, Germany) was used to determine the wettability of the scaffolds. The average water contact angle values were recorded using deionized water (sessile drop method) in three parts of each scaffold after 10 seconds at room temperature (6).

Assessment of pH changes

Different scaffolds with the same weights were immersed in simulated body fluid (SBF) at 37°C and pH=7.4 for one month. The pH of the solution was measured at different time intervals (7, 14, 21, and 30 days) using a Mettler Toledo pH metre (Greifensee, Switzerland) (6).

Hemocompatibility

Fresh human blood (2 ml) that contained the appropriate anticoagulant was diluted with normal saline (2.5 ml) to evaluate the blood compatibility of the scaffold. Three replications of each sample were placed in 96-well plate. Diluted blood (0.2 ml) was added to each well and the plate was placed in an incubator at 37°C for one hour. In the next step, the plate was centrifuged for 10 minutes at 1500 $\times g$. The absorbance of the sample was measured at 545 nm using an Anthos Microplate Reader (Biochrom, Berlin, Germany) by transferring the supernatant to a different 96-well plate. Normal saline (4 ml) with diluted blood (0.2 ml) was used as the negative control. The positive control sample consisted of 4 ml of distilled water with 0.2 ml of diluted blood (20). The following equation was used to calculate hemolysis:

$$\text{Hemolysis \%} = (Dt - Dnc) / (Dpc - Dnc) \times 100$$

Where Dt, Dpc, and Dnc are the absorption of the sample, positive control, and negative control, respectively.

Blood clotting index

The samples were cut into disk shapes and placed in beakers. Then, the beakers were placed in a 37°C water bath for one hour. Next, we added 100 μl of blood that contained the anticoagulant to each sample. After five minutes, 20 μl of 0.2 mol/l calcium chloride solution was added. After five minutes, 25 ml of distilled water was gently added to the samples. The samples were kept at 37°C for five minutes. Finally, their absorbance was measured at 545 nm. The control group included 100 μl of blood along with 25 ml of distilled water (no sample). The blood clotting index (BCI) was calculated according to the following equation:

$$\text{BCI} = A_{\text{sample}} / A_{\text{control}} \times 100\%$$

Where A_{sample} is the absorbance value of each sample and A_{control} is the absorbance value of the control group (21).

Compressive strength evaluation

The mechanical properties of the scaffolds were measured under dry and wet conditions at room temperature using a mechanical testing machine (Zwick Roell, Germany) with a 2N load cell and a speed of one mm/minute. The scaffolds were immersed in phosphate-buffered saline (PBS) for one hour to evaluate the mechanical properties under wet conditions. The samples were subjected to an increasing load until the strain reached 30%. The samples were cut into cylinders with a diameter and height of eight mm. Each test was repeated three times (22).

In vitro release profile of rosuvastatin

We evaluated the RSV release profile by placing the scaffolds in 10 ml of SBF on a shaker located in an incubator at 37°C. At specific time points (1, 2, 3, 6,

12, 18, and 30 days), the supernatants were collected and the same volume of fresh SBF was added to the scaffolds. The concentration of RSV was measured using a UV spectrophotometer (Cole-Parmer UV/Visible spectrophotometer, USA) at a wavelength of 240 nm (10).

MTT assay

The direct MTT test was used to evaluate the cytotoxicity of the scaffolds. The scaffolds were sterilized by ultraviolet radiation at 254 nm (20 minutes on each side). Human umbilical cord mesenchymal stem cells (HUC-MSCs) were isolated from umbilical cord blood bags according to a previous study procedure (23) and used for this experiment. We placed the sterile scaffolds (with three replicates) in 96-well plate and then added 1×10^4 cells to each well. The cells were incubated for 24 and 72 hours at 37°C. The MTT solution in PBS (5 mg/ml) was added to each well at a specific time point and the plates were incubated at 37°C for 4 hours. A total of 150 μ l of DMSO was added to each well to dissolve the formazan. Again, the plate was placed in a shaker incubator (in the dark) at 37°C for 20 minutes. A microplate reader (Biochrom GmbH, Berlin, Germany) set at a wavelength of 570 nm was used to record the absorbance of the resultant solution in each well (10). The following formula was used to calculate the survival percentage:

$$\text{survival percentage} = \text{ODe} / \text{ODb} \times 100$$

Where ODe is the optical density of the sample, and ODb is the optical density of the blank.

Alkaline phosphatase activity

ALP is a biochemical marker of osteoblasts that increases after osteogenic differentiation of HUC-MSCs (19). The scaffolds were sterilized with ultraviolet radiation at 254 nm (20 minutes on each side) and placed in 48-well plate. Then, 10^4 cells per well of HUC-MSCs were seeded on the scaffolds. The scaffolds were incubated in osteogenic medium (Bio Idea Company, Tehran, Iran) for 21 days. This medium includes dexamethasone, sodium pyruvate, beta glycerol phosphate, and ascorbic acid in Dulbecco's Modified Eagle's Medium-Low Glucose medium that contained foetal bovine serum. The cells were continuously checked and the medium was replaced. ALP activity was evaluated according to the manufacturer's instructions in the ALP kit (Delta. DP, Tehran, Iran). Briefly, on day 21, the scaffolds were washed twice with PBS and placed in 500 μ l TritonX-100 (1%) for 30 minutes at 37°C. The cell lysate was collected and centrifuged at $3000 \times g$ at 4°C for 15 minutes. Then, 100 μ l of the supernatant was transferred to a new microtube and the ALP premix solution (4:1 ratio of A:B solution) was added. After one- and 30-minutes incubation at 37°C, the absorbance of each sample was measured by a microplate reader at 405 nm. The amount of total protein was measured by the Bicinchoninic Acid Assay kit (BCA, DNA Biotech, Tehran, Iran) according to the manufacturer's protocol. We placed 25 μ l of each sample in the wells of 96-well plate

(three duplications), and 75 μ l of reagent (1:49 copper reagent to BCA reagent) was added. The plate was slowly shaken and incubated at 60°C for 60 minutes. The plates were cooled to room temperature, and the absorbance was measured at 562 nm. ALP activity values were normalized in terms of total protein.

Statistical analysis

GraphPad Prism software version 9 (GraphPad Software, Inc., USA) was used for statistical analysis. Data analysis was performed with one-way ANOVA, two-way ANOVA, and Tukey's post hoc test for different groups (with three repetitions). $P < 0.05$ indicate statistical significance. Low variables are described with mean and standard deviation.

Results

Fourier transform infrared spectroscopy

Figure 1 shows the Fourier transform infrared spectroscopy (FTIR) spectra for the scaffolds. The PCL-Gelatin-0 mg/10 ml RSV scaffold (black spectra) revealed characteristic peaks of PCL and gelatin: a peak at 2956 cm^{-1} (CH_2 asymmetrical stretching), 2863 cm^{-1} (CH_2 symmetrical stretching), 1731 cm^{-1} (carbonyl group), 1642 cm^{-1} (amide I bond), and 1260-1400 cm^{-1} (hydroxyl group). The addition of RSV revealed characteristic peaks at 3372 cm^{-1} (hydroxyl stretching), 1554 cm^{-1} (aromatic $\text{c}=\text{c}$ stretching), and 1440 and 1370 cm^{-1} (C-H bending) in the scaffolds that had various concentrations of RSV. This indicates the preservation of the RSV structure during the manufacturing process. The RSV bands became sharper with increasing concentrations of RSV. In addition, the position and intensity of the peaks also changed due to the hydrogen bond between the scaffold's components and RSV.

Scanning electron microscope

Figure 2 shows SEM images of the scaffolds' cross-sections. The scaffolds had well-defined internal geometry, highly porous structure, and proper pore connectivity. The pore size of the scaffolds increased with increased RSV concentration, from $34 \pm 4 \mu\text{m}$ in the PCL-Gelatin-0 mg/10 ml RSV scaffold to $81 \pm 1.8 \mu\text{m}$ in the PCL-Gelatin-62.5 mg/10 ml RSV scaffold.

Porosity assessment

Table 1 shows the percent of porosity of all the assessed scaffolds. The presence of the RSV did not cause any significant change in the percent of porosity of the scaffolds. In general, the scaffolds have sufficient porosity for the migration, growth, and proliferation of bone cells.

Weight loss assessment

Figure 3A shows the results of the degradation rate of various scaffolds at 7, 14, 21, and 30 days. The results show an increase in degradation rate over time. In addition, increasing the concentration of RSV, which is hydrophilic, can increase the degradation rate. However, the lower concentrations of RSV did not have a significant effect on the degradation rate.

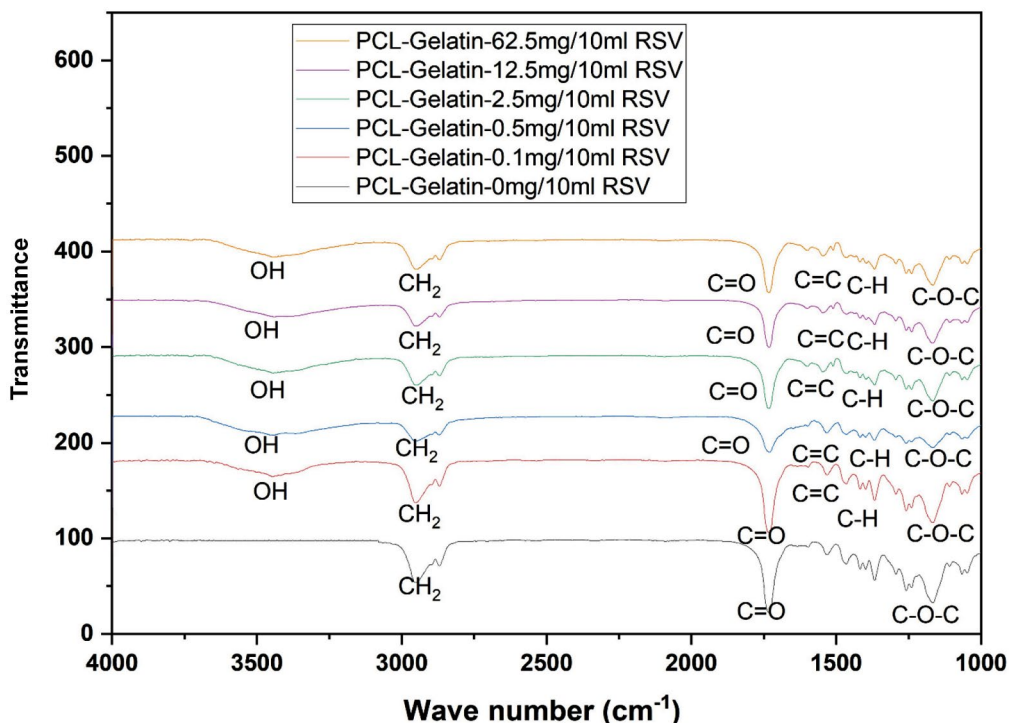


Fig.1: Functional groups or surface chemical bonds on the scaffolds. FTIR spectra of the PCL-Gelatin-0 mg/10 ml RSV (black spectra), PCL-Gelatin-0.1 mg/10 ml RSV (red spectra), PCL-Gelatin-0.5 mg/10 ml RSV (blue spectra), PCL-Gelatin-2.5 mg/10 ml RSV (green spectra), PCL-Gelatin-12.5 mg/10 ml RSV (purple spectra), and PCL-Gelatin-62.5 mg/10 ml RSV (orange spectra) scaffolds. The presence of gelatin, PCL, and the RSV functional groups indicates the stability of the components during the fabrication process. FTIR; Fourier transform infrared spectroscopy, PCL; Polycaprolactone, and RSV; Rosuvastatin.

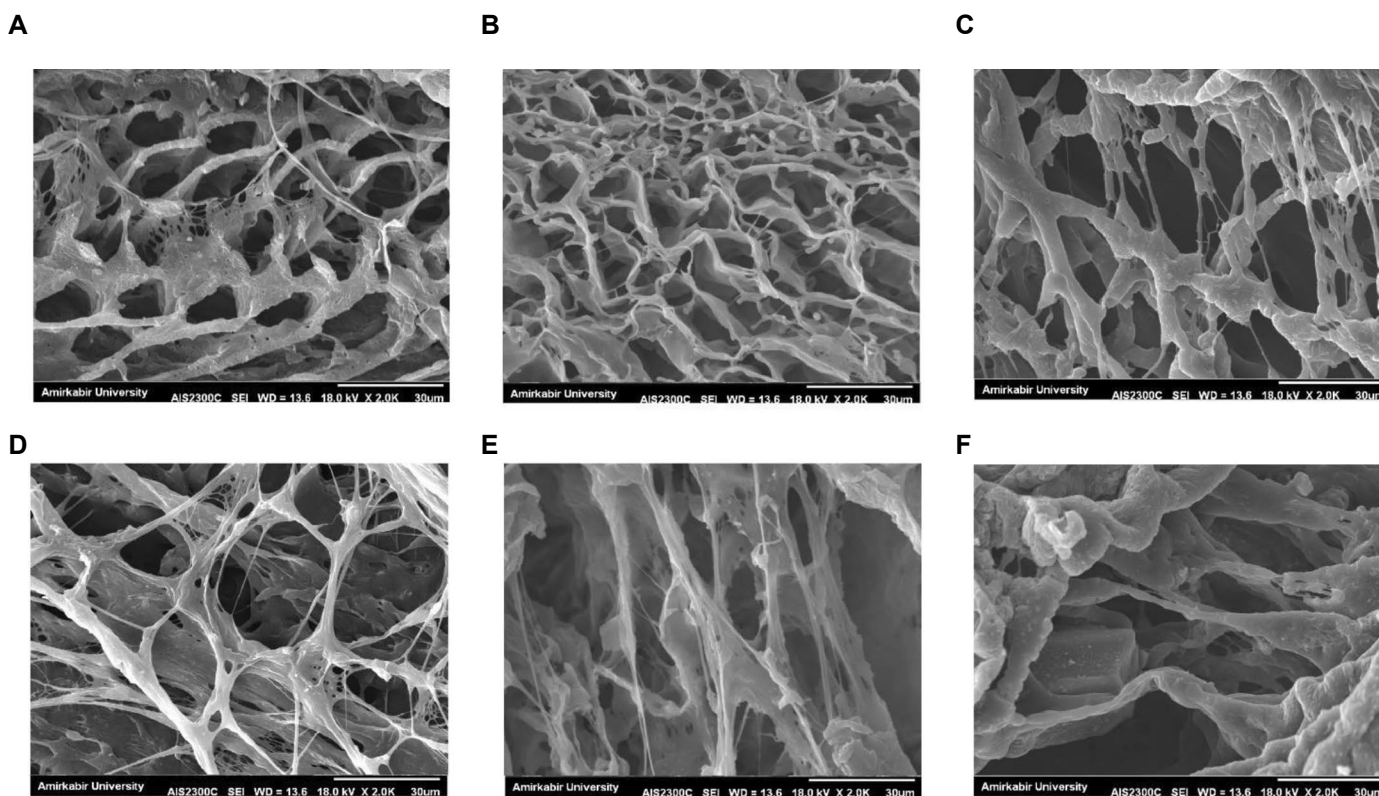


Fig.2: Morphological evaluation of scaffolds. **A.** SEM images of the PCL-Gelatin-0 mg/10 ml RSV, **B.** PCL-Gelatin-0.1 mg/10 ml RSV, **C.** PCL-Gelatin-0.5 mg/10 ml RSV, **D.** PCL-Gelatin-2.5 mg/10 ml RSV, **E.** PCL-Gelatin-12.5 mg/10 ml RSV, and **F.** PCL-Gelatin-62.5 mg/10 ml RSV scaffolds. Increases in the RSV concentration cause an increase in pore size. SEM; Scanning electron microscope, PCL; Polycaprolactone, and RSV; Rosuvastatin.

Table 1: Physical characteristics of the scaffolds

Sample	Porosity (%)	Compressive strength	Young's modulus	Compressive strength	Young's modulus	Pore size (μm)
		Dry (MPa)	Dry (MPa)	Wet (MPa)	Wet (MPa)	
PCL-Gelatin-0 mg/10 ml RSV	78 \pm 1.4	5.8 \pm 0.34	5.33 \pm 1.5	5.68 \pm 0.47	4.9 \pm 0.98	34 \pm 4
PCL-Gelatin-0.1 mg/10 ml RSV	78 \pm 3.2	6.19 \pm 1.35	5.39 \pm 0.89	6.01 \pm 0.14	4.9 \pm 0.37	34.12 \pm 2.1
PCL-Gelatin-0.5 mg/10 ml RSV	78 \pm 6.7	6.72 \pm 0.97	7 \pm 0.2	6.34 \pm 0.67	6.1 \pm 1.21	37.92 \pm 0.35
PCL-Gelatin-2.5 mg/10 ml RSV	79 \pm 0.3	11.23 \pm 0.47	10.22 \pm 2.63	10.34 \pm 1.02	9.76 \pm 0.9	46 \pm 5.4
PCL-Gelatin-12.5 mg/10 ml RSV	79 \pm 0.87	14.264 \pm 2.1	18.37 \pm 0.95	12.02 \pm 2.12	17.03 \pm 0.81	62.11 \pm 2.78
PCL-Gelatin-62.5 mg/10 ml RSV	79 \pm 2.2	16.342 \pm 1.79	24 \pm 0.14	13.86 \pm 2.62	22.73 \pm 0.15	81 \pm 1.8

Data are presented as mean \pm SD. PCL; Polycaprolactone and RSV; Rosuvastatin.

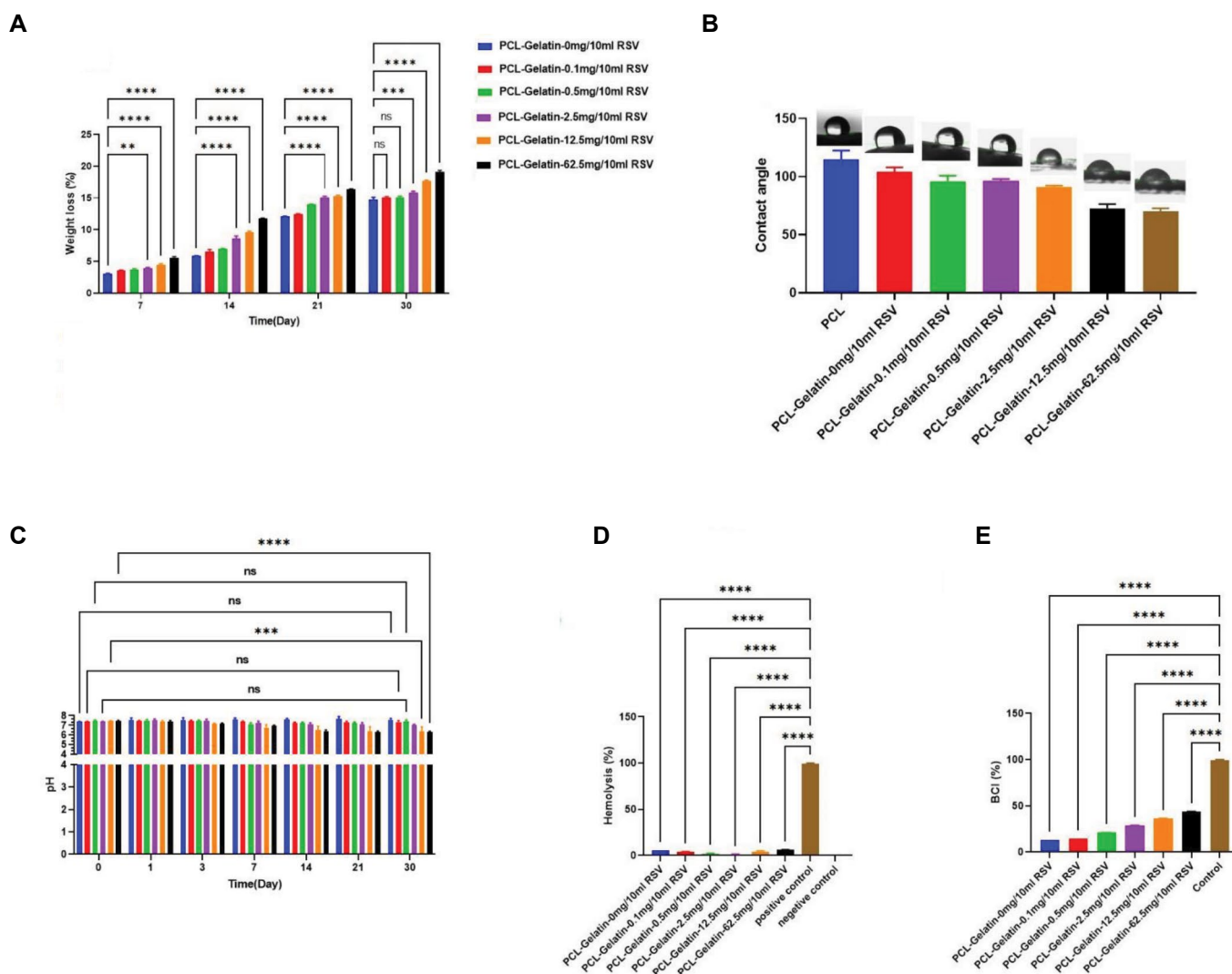


Fig.3: Evaluation of RSV effect on various properties of scaffolds. **A.** Evaluation of the scaffold degradation rate after 7, 14, 21, and 30 days. **B.** The contact angle of the PCL-gelatin scaffolds that contain different concentrations of RSV. **C.** pH changes of aqueous media in contact with the scaffolds after 7, 14, 21, and 30 days. **D.** Hemolysis percent and **E.** BCI of the scaffolds (mean \pm standard deviation, **, $P < 0.05$, ***, $P < 0.001$, and ****, $P < 0.0001$). RSV improved the degradation rate, wettability, and hemocompatibility of the scaffolds in a concentration-dependent manner. PCL; Polycaprolactone, RSV; Rosuvastatin, and BCI; Blood clotting index.

Wettability evaluation

As shown in Figure 3B, the addition of gelatin (as a hydrophilic component) to PCL decreased its contact angle from 118 to 101.7 degrees. In addition, the addition of RSV to the PCL-gelatin scaffold also reduced the contact angle in a concentration-dependent manner so that the PCL-Gelatin-62.5 mg/10 ml RSV scaffold had a contact angle equal to 70.2 degrees.

Assessment of pH changes

Figure 3C shows the pH changes of the aqueous medium (SBF) in contact with the scaffold after 7, 14, 21, and 30 days. More rapid pH changes occurred during the first two weeks, followed by a decreased rate of change. RSV acidified the pH of the environment, and this opposed the alkaline nature of gelatin.

Hemocompatibility

Figure 3D shows the hemolysis percent of the scaffolds. The hemolysis percent of all groups was significantly lower than the positive control, which indicated their hemocompatibility. The addition of up to 2.5 mg/10 ml RSV decreased hemolysis from 5.47 to 1.43%, which improved the hemocompatibility of the scaffolds. Higher amounts of RSV decreased the hemocompatibility.

Blood clotting index

Figure 3E shows the coagulation effect of the scaffolds according to the BCI. A lower BCI indicates a better coagulation effect and a faster coagulation rate. The drug-free scaffold had a BCI of 13.11. The addition of RSV (up to 62.5 mg/10 ml) increased this value to 43.8.

Compressive strength

The stress-strain curve and mechanical properties of the scaffolds are presented in Figure 4A and Table 1, respectively. Our results indicated that the RSV had a positive effect on the compressive strength of the scaffolds under both dry and wet conditions. The compressive strength increased from 5.8 ± 0.34 MPa for the PCL-Gelatin-0 mg/10 ml RSV scaffold to 16.342 ± 1.79 MPa for the PCL-Gelatin-62.5 mg/10 ml scaffold.

In vitro release profile of rosuvastatin

Figure 4B shows the RSV-release profile of the PCL-Gelatin-62.5 mg/10 ml RSV and PCL-Gelatin-2.5 mg/10 ml RSV scaffolds at 1, 2, 3, 6, 12, 18, and 30 days. According to the graph, there was a continuous release of RSV from the scaffold for 30 days; only $37 \pm 0.68\%$ (62.5 mg/10 ml RSV) and $31.68 \pm 1.02\%$ (2.5 mg/10 ml RSV) of the drug was released during this period. The scaffolds had a burst release during the first 12 days, which was related to the drug released in the surface pores of the scaffold. After that, the release continued gradually

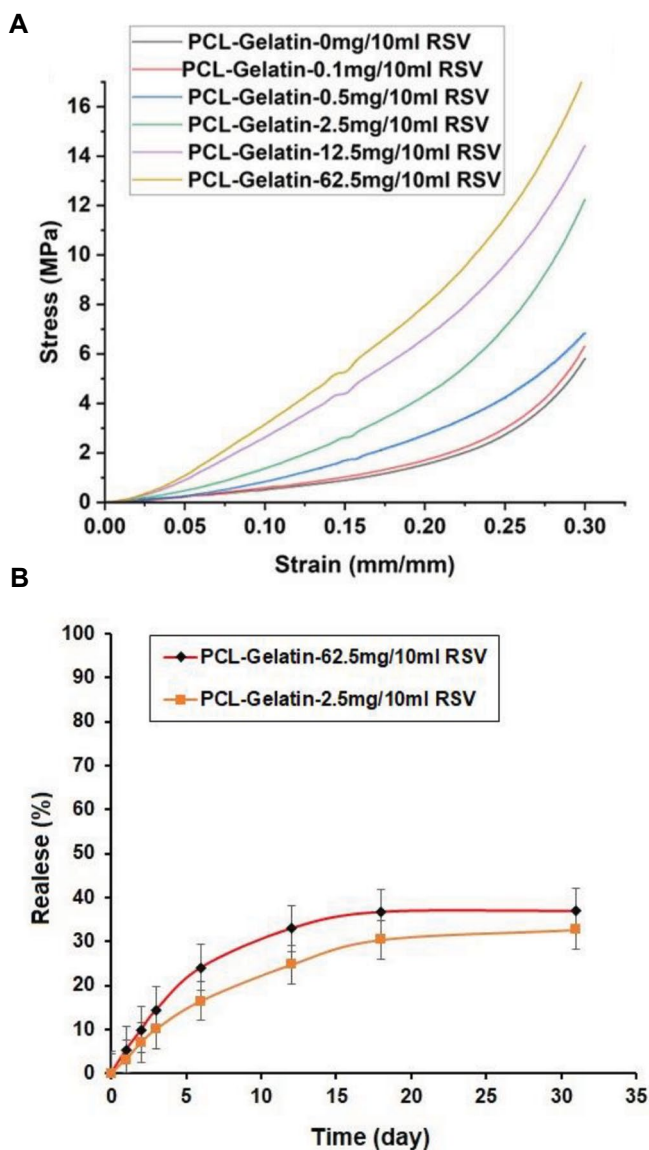


Fig.4: Evaluation of RSV effect on various properties of scaffolds. **A.** Stress-strain curves of the PCL-Gelatin-0 mg/10 ml RSV (black spectra), PCL-Gelatin-0.1 mg/10 ml RSV (red spectra), PCL-Gelatin-0.5 mg/10 ml RSV (blue spectra), PCL-Gelatin-2.5 mg/10 ml RSV (green spectra), PCL-Gelatin-12.5 mg/10 ml RSV (purple spectra), and PCL-Gelatin-62.5 mg/10 ml RSV (orange spectra) scaffolds under dry conditions indicate a positive effect of RSV on compressive strength. **B.** RSV release profile from the PCL-Gelatin-62.5 mg/10 ml RSV and PCL-Gelatin-2.5 mg/10 ml RSV scaffold within 30 days indicate sustained release of RSV (n=3). RSV: Rosuvastatin and PCL: Polycaprolactone.

We evaluated the data using different formulas and mathematical models related to each kinetic (zero-order, first-order, and Higuchi). Our results indicated that the kinetics of drug release was attributed to the zero-order model, in which the amount of RSV released at a certain time (Q_t) is calculated based on the initial amount of RSV in the solution (Q_0) according to the following equation:

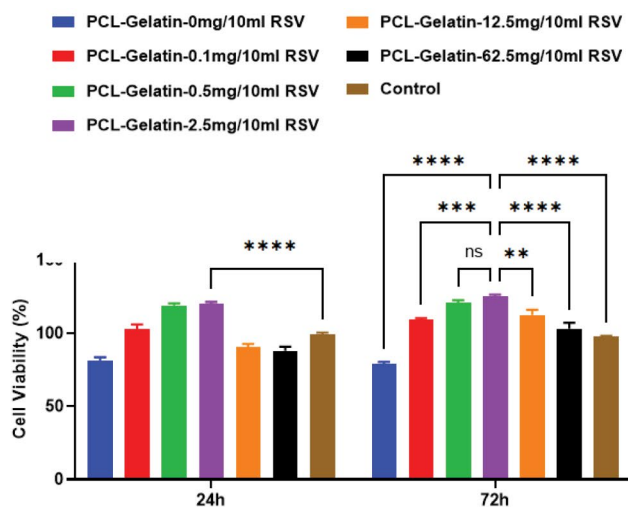
$$Q_t = Q_0 + k_0 t$$

Where k_0 is a rate constant. Zero-order kinetics results indicated that a constant amount of drug was released from the surface of the scaffold per unit of time. The release graph shows a straight line with a positive slope.

MTT assay

The cytotoxicity effect of these scaffolds on the survival of HUC-MSCs is shown in Figure 5A. We noted that increasing the amount of RSV to 2.5 mg/10 ml resulted in an increase in cell survival rate after 24 and 72 hours compared to the scaffolds without drugs. However, the 12.5 mg/10 ml and 62.5 mg/10 ml concentrations of RSV slightly reduced cell survival.

A



B

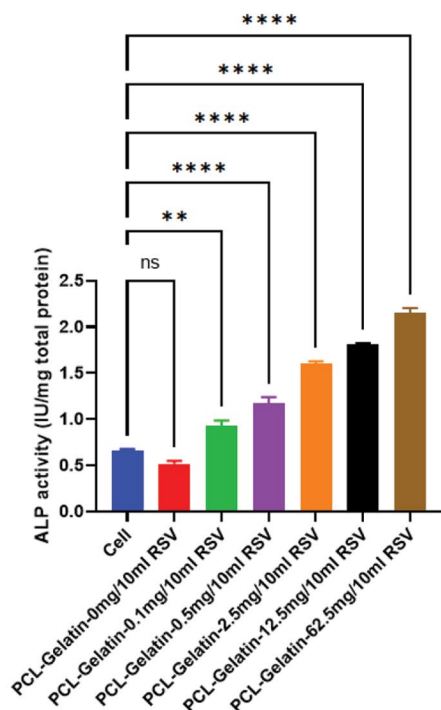


Fig. 5: Evaluation of RSV effect on biological properties of scaffolds. **A.** Cell viability assay of HUC-MSCs cultured on the scaffolds after 24 and 72 hours. **B.** ALP activity of MSCs after 21 days of culture with PCL-gelatin scaffolds that contain different concentrations of RSV (mean \pm standard deviation, **, $P < 0.05$, ***, $P < 0.001$, and ****, $P < 0.0001$). RSV improves the ALP activity of scaffolds in a concentration-dependent manner. MSCs; Mesenchymal stem cells, PCL; Polycaprolactone, RSV; Rosuvastatin, and ALP; Alkaline phosphatase.

Alkaline phosphatase activity

We evaluated the ALP activity to determine the osteogenic differentiation ability of the scaffolds that contained RSV. Figure 5B showed more ALP activity in the scaffolds that contained RSV compared to those without RSV and the sample without scaffold. Increasing RSV from 0.1 mg/10 ml to 62.5 mg/10 ml caused an approximately five-fold increase in ALP activity. RSV significantly increased osteogenic differentiation of the HUC-MSCs.

Discussion

The present study evaluated the PCL-gelatin-RSV scaffolds for use as a valuable tool for bone defect regeneration. We used the TIPS method to fabricate PCL-gelatin scaffolds that had different concentrations of RSV to assess the role of RSV in these scaffold characteristics.

RSV is a second-generation statin with seven to eight times the effectiveness of simvastatin and few side effects. It improves BMP-2 expression, ALP activity and bone formation, and delays osteoblastic apoptosis (17, 24). However, the primary metabolism of RSV in the liver has reduced its bioavailability after oral administration to less than 20%, and this does not have a good effect on osteogenesis. High doses of RSV cause an inflammatory response, cytotoxicity, and slow bone regeneration (11). Therefore, the preparation of suitable carriers for local administration of RSV can help to improve its performance, reduce side effects, and reduce the required dose.

In the present study, we used a PCL-gelatin composite as an RSV carrier for bone defect regeneration to take advantage of the positive effect of both components on bone tissue regeneration and ECM simulation. PCL is an inexpensive polymer with favourable mechanical properties of bone tissue, which is not desirable for use alone due to its hydrophobicity and low decomposition rate (7). Therefore, we used the PCL-gelatin combination to improve cell attachment and cell infiltration into the scaffold (more than 100 μm), create structures similar to trabecular bone, increase angiogenesis, and differentiate pre-osteoblast cells (8).

SEM images showed that the scaffolds had optimal interconnectivity and pore size to assist nutrient exchange, remove metabolites, and migrate bone cells. These scaffolds had about 78-79% porosity, which was in the range for cancellous bone (75-85%) and allowed the trabeculae matrix to penetrate the scaffold (25). The compressive strengths of the scaffolds were 5.8 ± 0.34 to 16.342 ± 1.79 MPa, which is in the optimal range for cancellous bone (1.5-45 MPa) and could prevent irritations and environmental damage (26).

The results of the drug release profile showed that only $31.68 \pm 0.1\%$ of the drug was released from the PCL-Gelatin-2.5 mg/10 ml RSV scaffold after 30 days, which indicated the potential of this system for slow,

local release of RSV. Therefore, these scaffolds could help bone regeneration during this period by making available a sufficient amount of RSV to the cells in the defect area. The resulting scaffolds had interconnected pores and uniform pore size, which made it possible to control degradation rate, porosity, pH changes, and pore size by changing the ratio of the components (PCL-gelatin) (6). The scaffolds created a desirable tool for the continuous release of RSV; however, previous studies did not achieve this release profile. Monjo et al. (13) used a resorbable collagen sponge impregnated with RSV, which was fixed in the defect by a titanium implant in order to repair bone defects in rabbit tibia. The collagen sponges released 82.5% of the drug in only 24 hours, which caused toxicity and reduced bone volume at higher doses and caused insufficient drug availability to the healing cells during the treatment period. The high concentrations of released RSV caused an excessive increase in BMP-2 expression and accelerated bone turnover, which did not leave enough time for bone mineralisation. Ibrahim and Fahmy (17) used polyelectrolyte sponges that consisted of chitosan-xanthan gum, polycarbophil, Carbopol®, and sodium alginate as a carrier for RSV to repair bone defects in rat femurs. They reported the release of 80% RSV from this carrier within eight hours.

We performed a cytotoxicity test to determine the biological effectiveness and optimal concentration of RSV loaded in the PCL-gelatin scaffolds because of the slow-release rate of RSV from these scaffolds. The results showed that the slow-release profile of RSV and its beneficial effects resulted in cell survival after 72 hours. However, concentrations above 2.5 mg/10 ml decreased cell survival. High concentrations of RSV prevent cholesterol production, which is an essential element for the maintenance of cell membrane integrity (16). Previous studies have shown that statins stimulate a cellular response and osteointegration, and their release kinetics can affect osteoblast differentiation (15). In agreement with our results, other groups have reported that concentrations of RSV greater than 10 μ M reduced cell survival (24).

In addition, our results showed that ALP activity in the HUC-MSCs increased with increasing RSV concentration, which confirmed the findings of previous studies (13). In their study, Monjo et al. (13) removed the collagen sponge from the rabbit tibia to examine ALP activity in the wound fluid. The results showed that the increase in RSV concentration increased ALP activity. Since the chemical composition and biological abilities of the scaffold affect cell behaviour, it can be stated that increasing the amount of RSV by improving the wettability of the scaffold would increase cell adhesion and differentiation (27). In addition, increasing the amount of RSV leads to improvements in the mechanical performance and stiffness of the scaffold, which facilitates osteogenic differentiation (28). In addition, RSV uses the Wnt/ β -catenin pathway for osteogenic differentiation of bone marrow-MSCs (in osteoporotic rats), which results in increased ALP activity.

RSV reduces the breakdown of β -catenin, increases its accumulation in cells, and stimulates the proliferation of osteoblasts (29). High ALP activity indicates early mineralisation and remodelling of bone tissue, and it decreases with the cessation of bone matrix deposition and mineralisation in mature osteocytes.

The results of the weight loss analysis indicate that the hydrophilic nature of RSV enables more water to penetrate the scaffold and increase hydrolysis (30). After one month, 62.5 mg/10 ml RSV increased the rate of scaffold degradation from $14.5 \pm 0.68\%$ to $19.8 \pm 1.37\%$. The scaffold degradation rate should be proportional to the bone regeneration rate (three months) and pure PCL has a degradation rate of 1.4% within 28 days (31), which may inhibit bone growth. Therefore, the presence of RSV could improve and impact the scaffold degradation rate.

The contact angle (wettability) of the scaffold is a critical parameter that determines the interaction of the scaffold with cells and proteins. According to previous studies, PCL has a high contact angle of about 118 degrees. Our results show that the addition of both gelatin and RSV, two hydrophilic components, to this scaffold helps to improve the contact angle and reduce the scaffold contact angles to 70.2 degrees, which enhances the cell-scaffold interaction.

Our evaluation of pH changes in this study showed the effect of the residues released from the scaffold during degradation on the surrounding environment. If these changes are excessive, they cannot be adjusted by the cells and result in toxicity (32). Our results showed drastic changes in pH in the first two weeks due to the release of di-hydroxy monocarboxylic acid (RSV) present in the surface pores. The presence of RSV partially neutralized the alkaline nature of the gelatin. During the initial days of bone mineralization, the accumulation of acidic metabolites results in a decrease in the pH of the tissue to less than normal serum. Then, with the precipitation of minerals and increasing calcium, the pH becomes more alkaline (33). By taking into consideration the essential role of tissue pH in bone repair and mineralisation, the residues released from the scaffold should not cause severe pH changes. In addition to its biocompatibility and favourable degradation rate, the scaffold that contained 2.5 mg/10 ml RSV also had small pH changes, which made it acceptable for bone tissue repair.

The amount of hemoglobin in the samples indicates the degree of red blood cell (RBC) membrane destruction. The hemolysis percent has an inverse relationship with the level of the scaffold's hemocompatibility. Generally, hemolysis up to 5% is acceptable for scaffolds (34). Previous studies have shown that statins can cause acute hemolysis, but RSV does not lead to hemolysis due to its structural difference with other statins (Atorvastatin and Lovastatin) (35). This is compatible with our results that showed a decrease in hemolysis with the addition of up to 2.5 mg/10 ml RSV. However, our results showed that higher amounts of RSV could increase hemolysis. The

cholesterol content of the RBC membrane is a factor that determines the mechanics of RBCs and the behaviour of their membranes. Statins can affect the cholesterol content of the RBC membrane, and their high amounts cause cell membrane rupture and increase hemolysis. In the case of atorvastatin, it has been proven that this statin can soften RBCs and increase the risk of hemolysis due to its shape and charge (36).

Blood coagulation on the implanted scaffold is one of the critical parameters in tissue regeneration. In damaged bone repair, the clot creates a temporary matrix that helps with cell absorption, migration, and bone repair. Blood clots induce maturation, differentiation, and repair of bone tissue (37). Our results show that high concentrations of RSV can reduce the rate of clot formation. Statins, as a weak anticoagulant factor, cause downregulation of the coagulation cascade and reduce the expressions of tissue factors and thrombin production. By inhibiting HMG-CoA reductase, they disrupt the coagulation reactions by this enzyme and activate the protein C anticoagulant pathway (38). However, the presence of PCL-gelatin moderates its effect to some extent by controlling the drug release rate and its coagulation properties. Tran (39) showed that the blood cells penetrated the PCL scaffold and caused clot strengthening. Furthermore, the new bone is also formed from the edge of the defect towards the centre of the scaffold, which shows the role of clot guidance. In total, the BCI index of the scaffolds that contained the highest concentration of RSV was 57% lower compared to the control group, which indicated that the scaffolds increased the blood coagulation rate, but low concentrations of RSV could be more effective.

Conclusion

This study evaluated the properties of PCL-gelatin scaffolds with different concentrations of RSV on bone healing. Our results show that the RSV had a dose-dependent positive effect on hydrophilicity, pore size, porosity, mechanical properties, weight loss, and hemocompatibility. The PCL-Gelatin-2.5 mg/10 ml RSV scaffolds have the best characteristics for BTE. The PCL-gelatin combination provides a favourable release system for RSV and greater bioavailability than free RSV.

Acknowledgements

This article was extracted from a Ph.D. dissertation and it was supported by grant no. 14010015 (Shahroud University of Medical Sciences). We sincerely thank Dr. Amir Atashi for supplying the MSCs for this research. There is no conflict of interest in this study.

Authors' Contributions

M.Gh.; Conceptualization, Formal analysis, Visualization, Resources, and Writing-original draft. M.A.; Conceptualization, Supervision, Investigation methodology, and Writing-original draft. M.K.F.; Resources, Investigation, and Writing-original draft.

M.S.; Conceptualization, Investigation, Methodology, Project administration, Supervision, and Writing-original draft. All of the authors have read and approved the paper for publication.

References

1. Ranjbarnejad F, Khazaei M, Shahryari A, Khazaei F, Rezakhani L. Recent advances in gene therapy for bone tissue engineering. *J Tissue Eng Regen Med*. 2022; 16(12): 1121-1137.
2. Murugan S, Parcha SR. Fabrication techniques involved in developing the composite scaffolds PCL/HA nanoparticles for bone tissue engineering applications. *J Mater Sci Mater Med*. 2021; 32(8): 93.
3. Gharibshahian M, Salehi M, Beheshtizadeh N, Kamalabadi-Farahani M, Atashi A, Nourbakhsh MS, et al. Recent advances on 3D-printed PCL-based composite scaffolds for bone tissue engineering. *Front Bioeng Biotechnol*. 2023; 11: 1168504.
4. Jang JW, Min KE, Kim C, Shin J, Lee J, Yi S. Scaffold characteristics, fabrication methods, and biomaterials for the bone tissue engineering. *Int J Precis Eng Manuf*. 2023; 24(3): 511-529.
5. Malikmammadov E, Tanir TE, Kiziltay A, Hasirci N. Preparation and characterization of poly(ϵ -caprolactone) scaffolds modified with cell-loaded fibrin gel. *Int J Biol Macromol*. 2019; 125: 683-689.
6. Hashemi SF, Mehrabi M, Ehterami A, Gharravi AM, Bitaraf FS, Salehi M. In-vitro and in-vivo studies of PLA/PCL/gelatin composite scaffold containing ascorbic acid for bone regeneration. *J Drug Deliv Sci Technol*. 2021; 61(4): 102077.
7. Ren K, Wang Y, Sun T, Yue W, Zhang H. Electrospun PCL/gelatin composite nanofiber structures for effective guided bone regeneration membranes. *Mater Sci Eng C*. 2017; 78: 324-332.
8. Sultana N, Hassan MI, Ridzuan N, Ibrahim Z, Soon CF. Fabrication of gelatin scaffolds using thermally induced phase separation technique. *Int J Eng*. 2018; 31(8): 1302-1307.
9. Wang CY, Hong PD, Wang DH, Cherng JH, Chang SJ, Liu CC, et al. Polymeric gelatin scaffolds affect mesenchymal stem cell differentiation and its diverse applications in tissue engineering. *Int J Mol Sci*. 2020; 21(22): 8632.
10. Akbari V, Rezazadeh M, Ebrahimi Z. Comparison the effects of chitosan and hyaluronic acid-based thermally sensitive hydrogels containing rosuvastatin on human osteoblast-like MG-63 cells. *Res Pharm Sci*. 2020; 15(1): 97-106.
11. Türer A, Coşkun Türer Ç, Durmuşlar MC, Ballı U, Önger ME. The influence of oral administration of rosuvastatin on calvarial bone healing in rats. *J Craniomaxillofac Surg*. 2016; 44(9): 1327-1332.
12. Türer A, Türer ÇÇ, Ballı U, Durmuşlar MC, Önger ME, Çelik HH. Effect of local rosuvastatin administration on calvarial bone defects. *J Craniofac Surg*. 2016; 27(8): 2036-2040.
13. Monjo M, Rubert M, Wohlfahrt JC, Rønold HJ, Ellingsen JE, Lyngstadaas SP. In vivo performance of absorbable collagen sponges with rosuvastatin in critical-size cortical bone defects. *Acta Biomater*. 2010; 6(4): 1405-1412.
14. Fan CH, Hao Y, Liu YH, Li XL, Huang ZH, Luo Y, et al. Anti-inflammatory effects of rosuvastatin treatment on coronary artery ectasia patients of different age groups. *BMC Cardiovasc Disord*. 2020; 20(1): 330.
15. Rezazadeh M, Parandeh M, Akbari V, Ebrahimi Z, Taheri A. Incorporation of rosuvastatin-loaded chitosan/chondroitin sulfate nanoparticles into a thermosensitive hydrogel for bone tissue engineering: preparation, characterization, and cellular behavior. *Pharm Dev Technol*. 2019; 24(3): 357-367.
16. Kalani MM, Nourmohammadi J, Negahdari B. Osteogenic potential of Rosuvastatin immobilized on silk fibroin nanofibers using argon plasma treatment. *Biomed Mater*. 2018 Dec 7; 14(2):025002.
17. Ibrahim HK, Fahmy RH. Localized rosuvastatin via implantable bioerodible sponge and its potential role in augmenting bone healing and regeneration. *Drug Deliv*. 2016; 23(9): 3181-3192.
18. Ehterami A, Abbaszadeh-Goudarzi G, Haghi-Daredeh S, Niyakan M, Alizadeh M, JafariSani M, et al. Bone tissue engineering using 3-D polycaprolactone/gelatin nanofibrous scaffold containing berberine: In vivo and in vitro study. *Polym Adv Technol*. 2022; 33(2): 672-681.
19. Kang YG, Wei J, Kim JE, Wu YR, Lee EJ, Su J, et al. Characterization and osteogenic evaluation of mesoporous magnesium-calcium silicate/polycaprolactone/polybutylene succinate composite scaffolds fabricated by rapid prototyping. *RSC Adv*. 2018; 8(59): 33882-33892.
20. Chi Perera CJ, Castillo Baas MG, Alcocer Lara GA, Ramos Borges

- SI, Rodríguez Guzmán AL, Fernández Cervantes I, et al. Characterization and hemocompatibility assessment of porous composite scaffolds with a biomimetic human clavicle macrostructure. *Health Technol.* 2020; 10: 423-428.
21. Zhang D, Hu Z, Zhang L, Lu S, Liang F, Li S. Chitosan-based thermo-sensitive hydrogel loading oyster peptides for hemostasis application. *Materials.* 2020; 13(21): 5038.
 22. Park HJ, Lee OJ, Lee MC, Moon BM, Ju HW, Lee Jm, et al. Fabrication of 3D porous silk scaffolds by particulate (salt/sucrose) leaching for bone tissue reconstruction. *Int J Biol Macromol.* 2015; 78: 215-223.
 23. Ajami M, Soleimani M, Abroun S, Atashi A. Comparison of cord blood CD34+ stem cell expansion in coculture with mesenchymal stem cells overexpressing SDF-1 and soluble /membrane isoforms of SCF. *J Cell Biochem.* 2019; 120(9): 15297-15309.
 24. Monjo M, Rubert M, Ellingsen JE, Lyngstadaas SP. Rosuvastatin promotes osteoblast differentiation and regulates SLC01A1 transporter gene expression in MC3T3-E1 cells. *Cell Physiol Biochem.* 2010; 26(4-5): 647-656.
 25. Novitskaya E, Chen PY, Lee S, Castro-Ceseña A, Hirata G, Lubarda VA, et al. Anisotropy in the compressive mechanical properties of bovine cortical bone and the mineral and protein constituents. *Acta Biomater.* 2011; 7(8): 3170-3177.
 26. Ait Said H, Noukrati H, Oudadesse H, Ben Youcef H, Lefevre B, Hakkou R, et al. Formulation and characterization of hydroxyapatite-based composite with enhanced compressive strength and controlled antibiotic release. *J Biomed Mater Res A.* 2021; 109(10): 1942-1954.
 27. Ghasemi-Mobarakeh L, Prabhakaran MP, Tian L, Shamirzaei-Jeshvaghani E, Dehghani L, Ramakrishna S. Structural properties of scaffolds: Crucial parameters towards stem cells differentiation. *World J Stem Cells.* 2015; 7(4): 728-744.
 28. Wang S, Hashemi S, Stratton S, Arinze TL. The effect of physical cues of biomaterial scaffolds on stem cell behavior. *Adv Healthc Mater.* 2021; 10(3): e2001244.
 29. Wang BX, Li KP, Yu T, Feng HY. Rosuvastatin promotes osteogenic differentiation of mesenchymal stem cells in the rat model of osteoporosis by the Wnt/ β -catenin signal. *Eur Rev Med Pharmacol Sci.* 2019; 23(22): 10161-10168.
 30. Stewart SA, Domínguez-Robles J, McIlorum VJ, Gonzalez Z, Utomo E, Mancuso E, et al. Poly(caprolactone)-based coatings on 3D-printed biodegradable implants: a novel strategy to prolong delivery of hydrophilic drugs. *Mol Pharm.* 2020; 17(9): 3487-3500.
 31. Wu F, Wei J, Liu C, O'Neill B, Ngothai Y. Fabrication and properties of porous scaffold of zein/PCL biocomposite for bone tissue engineering. *Compos B Eng.* 2012; 43(5): 2192-2197.
 32. Sung HJ, Meredith C, Johnson C, Galis ZS. The effect of scaffold degradation rate on three-dimensional cell growth and angiogenesis. *Biomaterials.* 2004; 25(26): 5735-5742.
 33. Berkmann JC, Herrera Martin AX, Ellinghaus A, Schlundt C, Schell H, Lippens E, et al. Early pH changes in musculoskeletal tissues upon injury-aerobic catabolic pathway activity linked to inter-individual differences in local pH. *Int J Mol Sci.* 2020; 21(7): 2513.
 34. Archana D, Singh BK, Dutta J, Dutta PK. In vivo evaluation of chitosan-PVP-titanium dioxide nanocomposite as wound dressing material. *Carbohydr Polym.* 2013; 95(1): 530-539.
 35. Moghadasi M, Maghsoomi Z. Statins can lead to acute hemolysis. *Cardiovasc Hematol Agents Med Chem.* 2018; 16(2): 123.
 36. Sheikh-Hasani V, Babaei M, Azadbakht A, Pazoki-Toroudi H, Mashaghi A, Moosavi-Movahedi AA, et al. Atorvastatin treatment softens human red blood cells: an optical tweezers study. *Biomed Opt Express.* 2018; 9(3): 1256-1261.
 37. Milillo L, Cinone F, Lo Presti F, Lauritano D, Petrucci M. The role of blood clot in guided bone regeneration: biological considerations and clinical applications with titanium foil. *Materials (Basel).* 2021; 14(21): 6642.
 38. Stępień K, Siudut J, Koniecznyńska M, Nowak K, Zalewski J, Undas A. Effect of high-dose statin therapy on coagulation factors: Lowering of factor XI as a modifier of fibrin clot properties in coronary artery disease. *Vascul Pharmacol.* 2023; 149: 107153.
 39. Tran PA. Blood clots and tissue regeneration of 3D printed dual scale porous polymeric scaffolds. *Mater Lett.* 2021; 285: 129184.